# WIDEBAND ROBUST BEAMFORMING BASED ON WORST-CASE PERFORMANCE OPTIMIZATION

*Amr El-Keyi*[†] *Thia Kirubarajan*[†] *Alex B. Gershman*[*]

[†]McMaster University
Department of Electrical and Computer Engineering
Hamilton, Ontario, Canada

[*]Darmstadt University of Technology
Communication Systems Group
Darmstadt, Germany

## ABSTRACT

A novel wideband beamformer is proposed with robustness against array response errors. The proposed beamformer differs from earlier techniques in that its robustness is directly related to the uncertainties in the array manifold while avoiding the suboptimal subband decomposition approach. The wideband robust beamforming problem is formulated as a second-order cone programming (SOCP) convex optimization problem which can be solved efficiently in polynomial time using interior point methods. Simulation results show an improved performance of the proposed beamformer compared to earlier wideband robust beamforming techniques.

## 1. INTRODUCTION

One of the early algorithms for adaptive array processing of wideband signals is the linearly constrained minimum variance (LCMV) algorithm [1]. The LCMV algorithm minimizes the array output power subject to look direction constraints. These constraints preserve the signals arriving from the desired look direction that appear in phase after the presteering delay filters. However, in practical scenarios the array performance can be severely degraded due to mismatches in the presumed array manifold. These mismatches might result from look direction errors, array sensor location errors, presteering delays quantization effects and/or wavefront distortions, and their effect can be grouped into presteering mismatches. As a result, the desired signal components can not be perfectly phase aligned by the presteering delays, and, thus, they are "interpreted" as interference and erroneously suppressed.

Several attempts have been made to add robustness to the wideband LCMV algorithm. An early work by Er and Cantoni presented a set of sufficient directional derivative constraints which can combat look direction errors [2]. More recently, additional first-order necessary and sufficient presteering delays (NS1-PS) derivative constraints were derived in [3]. These constraints were shown to be able to maintain array robustness despite the aforementioned array response errors. Similarly, diagonal loading [4]-[5] can add robustness to the LCMV algorithm. However, the amount of robustness provided in all these algorithms is set in an ad-hoc way and is not related to the amount of uncertainty in the array manifold.

Recently, several theoretically rigorous algorithms have been proposed to add robustness to the narrowband minimum variance (MV) beamformer so that it is matched to the amount of uncertainty in the array manifold [6], [7]. Related techniques for the wideband case have been presented in [8], where a suboptimal subband processing based constant power robust MV beamformer (CPRMVB) was presented.

In this paper, we propose a novel robust wideband beamformer with robustness directly linked to the level of uncertainty in the array manifold. It extends the work in [6] to the wideband case and avoids the suboptimal subband decomposition approach. Our beamformer maintains a high gain response not only to the signals appearing in phase after the presteering delays but also to all the signals with an additional norm-bounded phase error vector. The phase response of the array is controlled through additional linear phase constraints imposed on each of the finite impulse response (FIR) filters of the array processor. The result-

This work was supported in parts by the Wolfgang Paul Award Program of the Alexander von Humboldt Foundation (Germany) and German Ministry of Education and Research; Premier's Research Excellence Award Program of the Ministry of Energy, Science, and Technology (MEST) of Ontario; Natural Sciences and Engineering Research Council (NSERC) of Canada; and Communication and Information Technology Ontario (CITO).

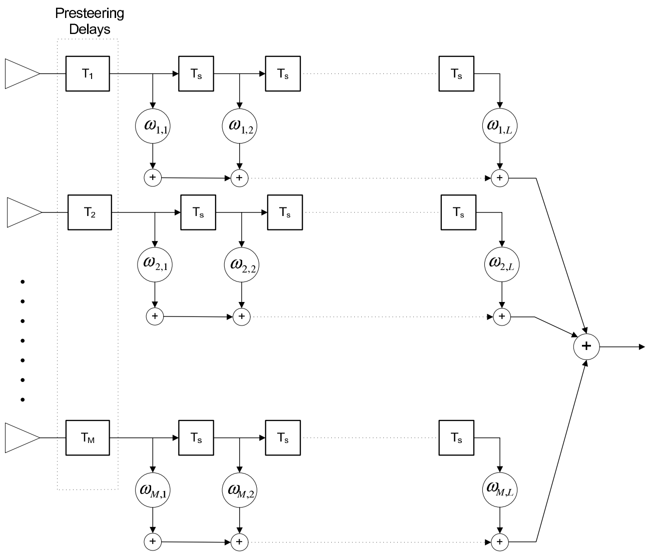


**Fig. 1**. Presteered broadband array processor.

ing problem is solved using the worst-case performance optimization approach and is shown to be convex. Simulation results verify that the proposed beamformer has an improved robustness against mismatches in array manifold as compared to other beamforming techniques.

## 2. ROBUST WIDEBAND BEAMFORMER

Consider an $M$-sensor $L$-tap presteered broadband array processor with $\omega_{m,l}$ denoting the weight at the $l$th tap of the $m$th FIR filter as shown in Figure 1. The sensors are uniformly spaced with an inter-element spacing less than or equal to $c/(2f_u)$, where $f_u$ is the maximum frequency of the desired signal and $c$ is the wave propagation speed. The received signal from the $i$th sensor is an input to a presteering delay $T_i$, whose output is sampled with the sampling frequency $f_s = 1/T_s$ where $f_s$ is selected greater than or equal to $2f_u$.

The $ML \times 1$ stacked snapshot vector containing $L$ delayed received data vectors is denoted by $\boldsymbol{x}(n)$. The $n$th sample of the beamformer output $y(n)$ is given by

$$y(n) = \boldsymbol{w}^T \boldsymbol{x}(n) \quad (1)$$

where $\boldsymbol{w}$ is the real valued $ML \times 1$ stacked weight vector, i.e., $\boldsymbol{w}_{M(l-1)+m} = \omega_{m,l}$, and $(\cdot)^T$ denotes the matrix transpose.

The response of the array to a complex sinusoid with frequency $f$ and arrival angle $\theta$ (where $\theta$ is measured with respect to the normal direction to the array aperture) is given by

$$H(f,\theta) = \boldsymbol{w}^T \left(\boldsymbol{d}(f) \otimes (\boldsymbol{T}(f)\boldsymbol{a}(f,\theta))\right) \quad (2)$$

where $\otimes$ denotes the Kronecker product,

$$\begin{aligned} \boldsymbol{d}(f) &= [1, e^{-j2\pi f T_s}, \ldots, e^{-j2\pi f(L-1)T_s}]^T & (3)\\ \boldsymbol{T}(f) &= \text{diag}\{e^{-j2\pi f T_1}, \ldots, e^{-j2\pi f T_M}\} & (4)\\ \boldsymbol{a}(f,\theta) &= [e^{j2\pi f \tau_1(\theta)}, \ldots, e^{j2\pi f \tau_M(\theta)}]^T & (5)\\ \tau_i(\theta) &= \frac{z_i \sin(\theta)}{c} & (6) \end{aligned}$$

and $z_i$ is the $i$th sensor location.

The presteering delays are selected so that the desired signal arriving from the presumed look direction $\theta_0$ appears coherently at the output of the $M$ delays, that is,

$$\boldsymbol{T}(f)\boldsymbol{a}(f,\theta_0) = \mathbf{1}_M \quad (7)$$

and the array response towards the desired signal becomes

$$H(f,\theta_0) = \boldsymbol{w}^T\left(\boldsymbol{d}(f) \otimes \mathbf{1}_M\right) = \boldsymbol{w}^T \boldsymbol{C}_0 \boldsymbol{d}(f) \quad (8)$$

where $\boldsymbol{C}_0 = \boldsymbol{I}_L \otimes \mathbf{1}_M \in \mathbb{R}^{ML \times L}$, $\boldsymbol{I}_L$ is the $L \times L$ identity matrix, and $\mathbf{1}_M$ is the $M \times 1$ vector containing all ones.

The LCMV beamformer obtains the weight vector by solving the following problem

$$\min_{\boldsymbol{w}} \boldsymbol{w}^T \boldsymbol{R}_{\boldsymbol{xx}} \boldsymbol{w} \quad \text{s.t.} \quad \boldsymbol{C}_0^T \boldsymbol{w} = \boldsymbol{h}_0 \quad (9)$$

where $\boldsymbol{R}_{\boldsymbol{xx}} = E\{\boldsymbol{x}(n)\boldsymbol{x}^T(n)\}$ is the data covariance matrix, and $\boldsymbol{h}_0$ specifies the frequency response of the beamformer towards the look direction. For all-pass response and in the case of odd number of taps, $\boldsymbol{h}_0$ is selected as $\boldsymbol{e}_{L_c}$, where $\boldsymbol{e}_i$ is a vector of appropriate dimension containing all zeros except for 1 in the $i$th position, and $L_c$ is the central tap index, i.e., $L_c = (L+1)/2$.

In the presence of mismatches in the array manifold, the desired signal components can not be perfectly aligned by the presteering delays. Assume that the incoherency in the desired signal components appearing after the presteering delay filters can be represented by a norm-bounded vector $\boldsymbol{\Delta}(f) \in \mathcal{A}_\varepsilon(f)$, that is, the desired signal component with frequency $f$ arriving from the direction $\theta_s$ appears after the presteering delays as

$$\boldsymbol{T}(f)\boldsymbol{a}(f,\theta_s) = e^{j2\pi f \varsigma}\mathbf{1}_M + \boldsymbol{\Delta}(f),\ \boldsymbol{\Delta}(f) \in \mathcal{A}_\varepsilon(f) \quad (10)$$

where $\varsigma$ is a common time delay at each of the $M$ sensors and the mismatch set $\mathcal{A}_\varepsilon(f)$ is defined as

$$\mathcal{A}_\varepsilon(f) = \{\boldsymbol{\Delta}(f) \in \mathbb{C}^{M\times 1} \mid \|\boldsymbol{\Delta}(f)\|_1 \le \varepsilon(f)\} \quad (11)$$

where $\|\cdot\|_i$ is the vector $i$-norm.

To prevent cancellation of the desired signal components, we impose a high gain constraint over the whole frequency band of the desired signal, i.e., $\forall f \in [f_l, f_u]$ and for all the received signal vectors with norm-bounded phase errors. This constraint can be written as

$$|H(f,\theta_s)| \ge 1 \quad \forall \boldsymbol{\Delta}(f) \in \mathcal{A}_\varepsilon(f); f \in [f_l, f_u]\,. \quad (12)$$

The optimal weight vector of the robust broadband beamformer can be obtained by minimizing the array output power $\boldsymbol{w}^T\boldsymbol{R_{xx}}\boldsymbol{w}$ subject to the above infinite set of constraints. Each constraint is imposed at a certain frequency $f$ and corresponds to the worst-case mismatch over $\mathcal{A}_\varepsilon(f)$ at this frequency. Thus, we can write (12) as

$$\min_{\boldsymbol{\Delta}(f)\in\mathcal{A}_\varepsilon(f)} |H(f,\theta_s)| \geq 1 \quad \forall f\in[f_l,f_u]\,. \tag{13}$$

In the presence of phase errors with the form in (10), the array response towards the desired signal is given by

$$H(f,\theta_s) = e^{j2\pi f\varsigma}\boldsymbol{w}^T\boldsymbol{C}_0\boldsymbol{d}(f) + \boldsymbol{w}^T\boldsymbol{Q}(f)\boldsymbol{\Delta}(f) \tag{14}$$

where $\boldsymbol{Q}(f)\in\mathbb{C}^{ML\times M} = \boldsymbol{d}(f)\otimes\boldsymbol{I}_M$. Using the triangle inequality we can write

$$|H(f,\theta_s)| \geq |\boldsymbol{w}^T\boldsymbol{C}_0\boldsymbol{d}(f)| - |\boldsymbol{w}^T\boldsymbol{Q}(f)\boldsymbol{\Delta}(f)|. \tag{15}$$

Maximizing the second term in the right hand side of (15) over the mismatch set $\mathcal{A}_\varepsilon(f)$ yields

$$\max_{\boldsymbol{\Delta}(f)\in\mathcal{A}_\varepsilon(f)} |\boldsymbol{w}^T\boldsymbol{Q}(f)\boldsymbol{\Delta}(f)| = \varepsilon(f)\|\boldsymbol{Q}^T(f)\boldsymbol{w}\|_\infty. \tag{16}$$

Combining (15) and (16), the minimum value of $|H(f,\theta_s)|$ over the mismatch set at the frequency $f$ is given by

$$\min_{\boldsymbol{\Delta}(f)\in\mathcal{A}_\varepsilon(f)} |H(f,\theta_s)| = |\boldsymbol{w}^T\boldsymbol{C}_0\boldsymbol{d}(f)| - \varepsilon(f)\|\boldsymbol{Q}^T(f)\boldsymbol{w}\|_\infty. \tag{17}$$

Thus, the robust beamforming problem can be written as

$$\begin{aligned}\min_{\boldsymbol{w}} \quad & \boldsymbol{w}^T\boldsymbol{R_{xx}}\boldsymbol{w}\\ \text{s.t.} \quad & |\boldsymbol{w}^T\boldsymbol{C}_0\boldsymbol{d}(f)| - \varepsilon(f)\|\boldsymbol{Q}^T(f)\boldsymbol{w}\|_\infty \geq 1\\ & \forall f\in[f_l,f_u]\end{aligned} \tag{18}$$

Note that $|\boldsymbol{w}^T\boldsymbol{C}_0\boldsymbol{d}(f)|$ and $\boldsymbol{Q}^T(f)\boldsymbol{w}$ can be expressed as

$$|\boldsymbol{w}^T\boldsymbol{C}_0\boldsymbol{d}(f)| = |\mathcal{W}_1(f)+\ldots+\mathcal{W}_M(f)| \tag{19}$$

$$\boldsymbol{Q}^T(f)\boldsymbol{w} = [\mathcal{W}_1(f),\ldots,\mathcal{W}_M(f)]^T \tag{20}$$

where $\mathcal{W}_m(f)$ is the frequency response of the $m$th FIR filter of the array processor.

The gain constraint in (12) can prevent the cancellation of the desired signal components, yet it does not guarantee a distortionless response because the phase response of the array towards the desired signal is completely unconstrained. To alleviate this problem, we impose a type 1 linear phase constraint on each of the $M$ FIR filters ($L$ must be odd) [9]. Although this constraint does not guarantee an overall linear phase response towards all the received signals, the overall response has nearly linear phase for the desired signal components with norm-bounded phase errors. In addition, the imposed linear phase constraints can be shown to be equivalent to NS1-PS derivative constraints in the case of an all-pass response. Therefore, they add more robustness to the beamformer.

Under the linear phase constraint, we can write the frequency response of the $m$th FIR filter as

$$\mathcal{W}_m(f) = \mathrm{e}^{-j\phi(f)}\Big(\omega_{m,L_c} + 2\sum_{k=L_c+1}^{L}\omega_{m,k}\cos(2\pi f(k-L_c)T_s)\Big) \tag{21}$$

where $\phi(f) = 2\pi f(L_c-1)T_s$.

Defining the vector $\boldsymbol{g}(f)\in\mathbb{R}^{L_c\times 1}$, and the matrices $\boldsymbol{C}_m\in\mathbb{R}^{ML\times L}$ and $\boldsymbol{B}\in\mathbb{R}^{L\times L_c}$ as

$$\boldsymbol{g}(f) \triangleq [1,\cos(2\pi fT_s),\ldots,\cos(2\pi f(L_c-1)T_s)]^T \tag{22}$$

$$\boldsymbol{C}_m \triangleq \boldsymbol{I}_L\otimes\boldsymbol{e}_m, \quad m=1,\ldots,M \tag{23}$$

$$\boldsymbol{B}^T \triangleq \begin{bmatrix} 0 & \cdots & 0 & 0 & 1 & 0 & 0 & \cdots & 0\\ 0 & \cdots & 0 & 1 & 0 & 1 & 0 & \cdots & 0\\ \vdots & & \iddots & & & & \ddots & & \vdots\\ 0 & 1 & 0 & & & & 0 & 1 & 0\\ 1 & 0 & 0 & & \cdots & & 0 & 0 & 1 \end{bmatrix} \tag{24}$$

we can rewrite (21) as

$$\mathcal{W}_m(f) = e^{-j\phi(f)}\boldsymbol{w}^T\boldsymbol{C}_m\boldsymbol{B}\boldsymbol{g}(f). \tag{25}$$

Also, using the fact that $\sum_{i=1}^M \boldsymbol{C}_i = \boldsymbol{C}_0$, we can write

$$\sum_{m=1}^M \mathcal{W}_m(f) = e^{-j\phi(f)}\boldsymbol{w}^T\boldsymbol{C}_0\boldsymbol{B}\boldsymbol{g}(f) \tag{26}$$

where $\boldsymbol{w}^T\boldsymbol{C}_m\boldsymbol{B}\boldsymbol{g}(f)$ and $\boldsymbol{w}^T\boldsymbol{C}_0\boldsymbol{B}\boldsymbol{g}(f)$ are real.

Therefore, the robust beamforming problem in (18) with the additional linear phase constraints can be written as

$$\begin{aligned}\min_{\boldsymbol{w},v} \quad & \boldsymbol{w}^T\boldsymbol{R_{xx}}\boldsymbol{w}\\ \text{s.t.} \quad & \omega_{m,L_c-l} = \omega_{m,L_c+l} && \forall m\in Z_1^M;\, l\in Z_1^{L_c-1}\\ & -v \leq \boldsymbol{w}^T\boldsymbol{C}_m\boldsymbol{B}\boldsymbol{g}(f) \leq v && \forall m\in Z_1^M;\, f\in[f_l,f_u]\\ & |\boldsymbol{w}^T\boldsymbol{C}_0\boldsymbol{B}\boldsymbol{g}(f)| - \varepsilon(f)v \geq 1 && \forall f\in[f_l,f_u]\end{aligned} \tag{27}$$

where $Z_i^j$ denotes the ring of integers from $i$ to $j$.

The problem is still nonconvex due to the absolute value operator in the last constraint. However, we can see that if $\{\boldsymbol{w},v\}$ is an optimal solution to the above optimization problem, then $\{-\boldsymbol{w},v\}$ is also an optimal solution. Also, examining the constraint $|\sum_{m=1}^M \mathcal{W}_m(f)| \geq 1+\varepsilon(f)v$ and from the continuity of the Fourier transform, it is clear that for a feasible weight vector $\boldsymbol{w}$, $e^{j\phi(f)}\sum_{m=1}^M \mathcal{W}_m(f)$ can either be positive or negative over the entire frequency band $[f_l,f_u]$ and can not change sign at any frequency. From these two remarks, it follows that imposing a nonnegativity constraint on the real valued phase-rotated sum of the

Fourier transforms of the $M$ FIR filters does not lead to any loss of optimality and yields the same global optimum solution of the nonconvex problem. Therefore, we can replace $|\boldsymbol{w}^T \boldsymbol{C}_0 \boldsymbol{B} \boldsymbol{g}(f)|$ in the last constraint of (27) by $\boldsymbol{w}^T \boldsymbol{C}_0 \boldsymbol{B} \boldsymbol{g}(f)$, and rewrite the constraint as $\boldsymbol{w}^T \boldsymbol{C}_0 \boldsymbol{B} \boldsymbol{g}(f) - \varepsilon(f)v \geq 1$. The resulting problem is a convex optimization problem.

The infinite set of spectral constraints imposed over the frequency interval $[f_l, f_u]$ can be represented in a finite manner using the standard discretization approach [10]. Therefore, the robust beamforming problem can be written as

$$\begin{aligned}
\min_{\boldsymbol{w},v} \;& \boldsymbol{w}^T \boldsymbol{R}_{\boldsymbol{xx}} \boldsymbol{w} \\
\text{s.t.}\; & \omega_{m,L_c-l} = \omega_{m,L_c+l} && \forall m \in Z_1^M; l \in Z_1^{L_c-1} \\
& \boldsymbol{w}^T \boldsymbol{C}_m \boldsymbol{B} \boldsymbol{g}(f_i) \leq v - \delta && \forall m \in Z_1^M; i \in Z_1^N \\
& \boldsymbol{w}^T \boldsymbol{C}_m \boldsymbol{B} \boldsymbol{g}(f_i) \geq -v + \delta && \forall m \in Z_1^M; i \in Z_1^N \\
& \boldsymbol{w}^T \boldsymbol{C}_0 \boldsymbol{B} \boldsymbol{g}(f_i) - \varepsilon(f_i)v \geq 1 + \delta && \forall i \in Z_1^N
\end{aligned} \tag{28}$$

where $\{f_i\}_{i=1}^N$ is a uniformly spaced grid selected over the band $[f_l, f_u]$, and $N$ and $\delta$ are chosen as follows. For a fixed $N$, one must choose $\delta$ small enough such that the over-constraining of the problem at the frequencies $f_i$ does not result in significant performance loss. At the same time, one must also choose $\delta$ large enough to satisfy the spectral constraints for all frequency components not included in the selected grid.

Next, we will convert the quadratic objective function into a linear one. Let

$$\boldsymbol{R}_{\boldsymbol{xx}} = \boldsymbol{U}^T \boldsymbol{U} \tag{29}$$

be the Cholesky factorization of $\boldsymbol{R}_{\boldsymbol{xx}}$. Thus, we can write the objective function as

$$\boldsymbol{w}^T \boldsymbol{R}_{\boldsymbol{xx}} \boldsymbol{w} = \|\boldsymbol{U}\boldsymbol{w}\|^2. \tag{30}$$

Obviously, minimizing $\|\boldsymbol{U}\boldsymbol{w}\|$ is equivalent to minimizing $\boldsymbol{w}^T \boldsymbol{R}_{\boldsymbol{xx}} \boldsymbol{w}$. Hence, introducing a scalar nonnegative auxiliary variable $t$, and imposing the additional constraint $\|\boldsymbol{U}\boldsymbol{w}\| \leq t$, we can convert (28) into the following SOCP problem:

$$\begin{aligned}
\min_{\boldsymbol{w},v,t} \;& t \\
\text{s.t.}\; & \|\boldsymbol{U}\boldsymbol{w}\| \leq t \\
& \omega_{m,L_c-l} = \omega_{m,L_c+l} && \forall m \in Z_1^M; l \in Z_1^{L_c-1} \\
& \boldsymbol{w}^T \boldsymbol{C}_m \boldsymbol{B} \boldsymbol{g}(f_i) \leq v - \delta && \forall m \in Z_1^M; i \in Z_1^N \\
& \boldsymbol{w}^T \boldsymbol{C}_m \boldsymbol{B} \boldsymbol{g}(f_i) \geq -v + \delta && \forall m \in Z_1^M; i \in Z_1^N \\
& \boldsymbol{w}^T \boldsymbol{C}_0 \boldsymbol{B} \boldsymbol{g}(f_i) - \varepsilon(f_i)v \geq 1 + \delta && \forall i \in Z_1^N
\end{aligned} \tag{31}$$

which can be solved efficiently using interior point methods [11]. The number of design variables is $ML+2$, and the first constraint is an $(ML+1)$-dimensional second-order cone constraint followed by $M(L_c-1)$ linear equality constraints and $(2M+1)N$ linear inequality constraints.

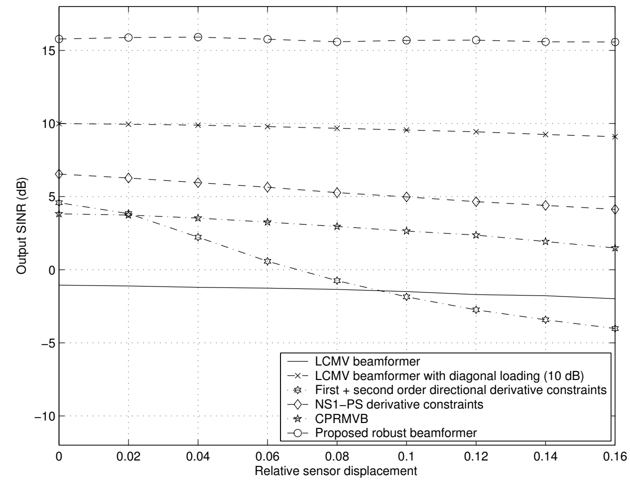


**Fig. 2**. Output SINR versus sensor location error.

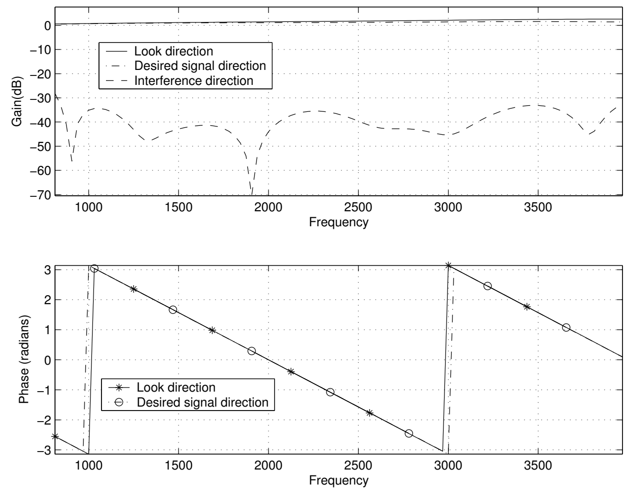


**Fig. 3**. Frequency response of the proposed robust beamformer.

The number of iterations required to solve an SOCP problem using interior point methods is bounded by the square root of the number of constraints [12]. The computational complexity associated with each iteration is of $\mathcal{O}(n^2 \sum_i q_i)$, where $n$ is the number of optimization variables and $q_i$ is the dimension of the $i$th constraint [12]. Therefore, the worst-case computational load of (31) will be of $\mathcal{O}(M^{3.5}L^2\zeta^{1.5})$ where $\zeta = \max\{N, L\}$. This computational complexity is comparable to the complexity of the classical LCMV algorithm which requires $\mathcal{O}(M^3L^3)$ operations to compute the inverse of the data covariance matrix [1].

## 3. SIMULATIONS

We consider a linear microphone array with $M = 10$ and $L = 9$. The sensors are assumed to be equispaced with spacing $c/f_s$, where $f_s = 8000$. The array is presteered to the direction $\theta_0 = -30^\circ$ and the presteering delays are quantized to 256 levels. The desired signal is a broadband signal arriving from the direction $\theta_s = -34^\circ$ with signal-to-noise ratio (SNR) equal to 10 dB and constant power spectral density over the frequency band 800–4000 Hz. A wideband interference signal is received from the direction $\theta_1 = 20^\circ$ with constant spectral density over the frequency band of interest and interference-to-signal ratio (ISR) equal to 20 dB. A uniformly-spaced frequency grid with $N = 11$ is selected to discretize the spectral constraints and a value of $\delta = 10^{-3}$ is chosen. The robustness set $\mathcal{A}_\varepsilon(f)$ is fixed throughout all simulations and is formed by considering a $2^\circ$ look direction error, $3.75\%$ sensor displacements relative to the array inter-element spacing, and steering delays quantization effects. A sample size of $N_s = 4096$ samples is used for the calculation of the sample correlation matrices for different beamformers. For the CPRMVB, 256 subbands are considered and the samples are divided into 16 batches. The correlation matrix of each subband is formed using the available 16 samples for that subband. The desired signal is chosen as a chirp signal $s(k) = \cos(2\pi f_l k T_s + \pi\beta k^2 T_s^2)$ with chirp rate $\beta = (f_u - f_l)/(N_s T_s)$, whereas the interference signal is generated as the sum of sinusoidal harmonics with random phases and equal powers occupying the band between $f_l$ and $f_u$. The simulation results are averaged over 100 independent runs.

We investigate the effect of sensor location errors. The actual sensor locations are selected such that they correspond to the maximum deformation in the linear array. We compare the performance of our robust beamformer with that of the classical LCMV beamformer and different robust beamformers with robustness provided through diagonal loading, directional derivative constraints, NS1-PS derivative constraints, and subband-based CPRMVB of [8].

Figure 2 shows the average output signal-to-interference-plus-noise ratio (SINR) for different relative sensor displacements from which we can clearly see improvements achieved by the proposed beamformer with respect to all other beamformers tested.

Figure 3 illustrates the frequency response of our beamformer for the case of $3.75\%$ of relative sensor displacement. The magnitude and phase responses are plotted at the presumed look direction and the actual desired signal direction. It is clear that our beamformer maintains a distortionless response and linear phase towards the desired signal in spite of the mismatches. Figure 3 also shows the magnitude response at the interference direction where we can see that the interference signal is suppressed at all frequencies.

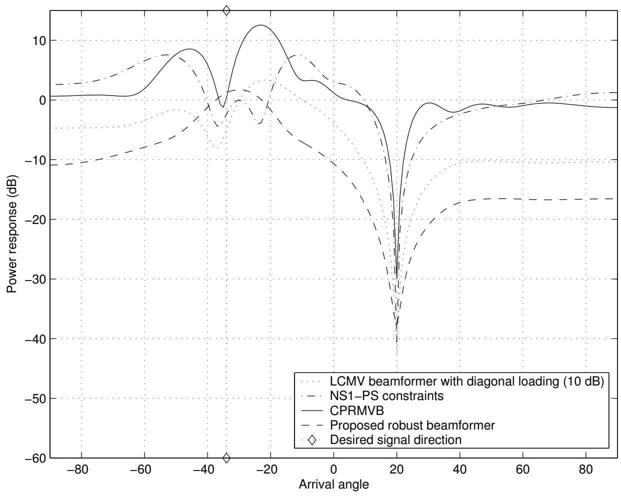


**Fig. 4**. Power response versus arrival angle.

Figure 4 shows the power response of various beamformers versus the arrival angle where we notice that our beamformer yields a high gain towards the desired signal while also suppressing the interference and maintaining a relatively low sidelobe level compared to other beamformers.

Next, we investigate the performance of our beamformer for different values of the desired signal SNR. The sensor displacements are $7.5\%$ of the sensor spacing, and ISR $=$ 0 dB. Figure 5 shows the output SINR for different beamformers versus the desired signal SNR. From this figure, we can see that our beamformer has a substantially improved performance as compared to the beamforming algorithms tested. These performance improvements are especially significant at high SNRs.

For the same scenario, we evaluate the normalized mean square error (NMSE) as well. Figure 6 shows the NMSE versus the desired signal SNR for different beamformers. We can observe that our robust beamformer provides dramatic improvements of the NMSE as compared to the other beamformers tested.

## 4. CONCLUSIONS

In this paper, a novel robust wideband adaptive beamformer has been presented. In contrast to earlier approaches, it provides an amount of robustness directly linked to the amount of uncertainty in the array manifold and aviods suboptimal subband decomposition. The proposed beamformer is demonstrated to prevent the cancellation of the desired signal through gain constraints imposed on all the received signal components within a certain predefined mismatch set. Linear phase constraints are also imposed to decrease phase distortions of the desired signal. The problem is formulated

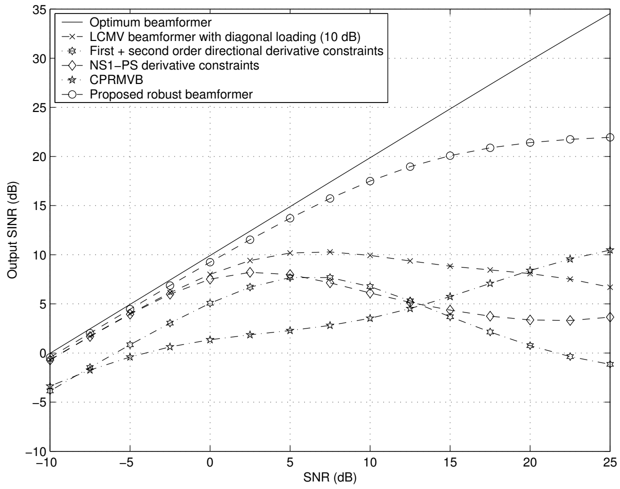


**Fig. 5**. Output SINR versus desired signal SNR.

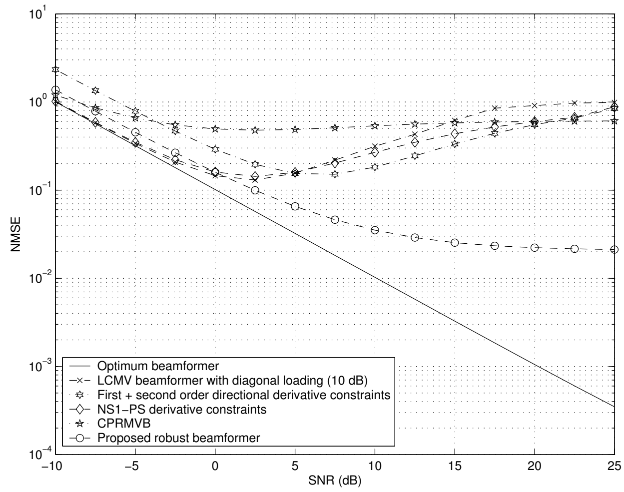


**Fig. 6**. NMSE versus desired signal SNR.

as a convex optimization problem which can be solved efficiently with polynomial complexity using well-established interior point methods. Simulation results validate a substantially improved performance of the proposed beamformer as compared to several popular robust wideband beamformers.

## 5. REFERENCES


[1] O. L. Frost III, "An algorithm for linearly constrained adaptive antenna array processing," *Proc. IEEE*, vol. 60, pp. 926–935, Aug. 1972.

[2] M. H. Er and A. Cantoni, "Derivative constraints for broad-band element space antenna array processors," *IEEE Trans. Acoust., Speech, Signal Processing*, vol. 31, pp. 1378–1393, Dec. 1983.

[3] S. Zhang and I. Thng, "Robust presteering derivative constraints for broadband antenna arrays," *IEEE Trans. Signal Processing*, vol. 50, pp. 1–10, Jan. 2002.

[4] Y. I. Abramovich, "Controlled method for adaptive optimization of filters using the criterion of maximum SNR," *Radio Engineering and Electronic Physics*, vol. 26, pp. 87-95, March 1981.

[5] H. Cox, R. M. Zeskind, and M. H. Owen, "Robust adaptive beamforming," *IEEE Trans. Acoust., Speech, Signal Processing*, vol. 35, pp. 1365–1376, Oct. 1987.

[6] S. A. Vorobyov, A. B. Gershman, and Z. Q. Luo, "Robust adaptive beamforming using worst-case performance optimization: a solution to the signal mismatch problem," *IEEE Trans. Signal Processing*, vol. 51, pp. 313–324, Feb. 2003.

[7] R. Lorenz and S. P. Boyd, "Robust minimum variance beamforming," *IEEE Trans. Signal Processing*, vol. 53, pp. 1684 – 1696, May 2005.

[8] Z. Wang, J. Li, P. Stoica, T. Nishida, and M. Sheplak, "Constant-beamwidth and constant-powerwidth wideband robust Capon beamformers for acoustic imaging," *J. Acoust. Soc. America*, vol. 116, pp. 1621–1631, Sept. 2004.

[9] T. W. Parks and C. S. Burrus, *Digital Filter Design*, John Wiley & Sons, New York, 1987.

[10] R. Hettich and K. O. Kortanek, "Semi-infinite programming: Theory, methods, and applications," *SIAM Rev.*, vol. 35, pp. 380–429, Sept. 1993.

[11] J. F. Strum, "Using sedumi 1.02, a matlab toolbox for optimization over symmetric cones," *Optim. Meth. Softw.*, vol. 11-12, pp. 625–653, Aug. 1999.

[12] M. Lobo, L. Vandenberghe, S. Boyd, and H. Lebret, "Applications of second-order cone programming," *Linear Alg. Applicat.*, vol. 284, pp. 193–228, Nov. 1998.